The Role of Surface Defects in CO Oxidation, Methanol Oxidation, and Oxygen Reduction on Pt (111)

Journal of The Electrochemical Society, **154** (12) F238-F242 (2007)
0013-4651/2007/154(12)/F238/5/$20.00 © The Electrochemical Society

The Role of Surface Defects in CO Oxidation, Methanol Oxidation, and Oxygen Reduction on Pt(111)

Jacob S. Spendelow,*,[a] Qinqin Xu, Jason D. Goodpaster, Paul J. A. Kenis, and Andrzej Wieckowski**,[z]**

Department of Chemistry and Department of Chemical and Biomolecular Engineering, University of Illinois at Urbana-Champaign, Urbana, Illinois 61801, USA

Some surface reactions of interest to electrocatalysis in alkaline media are promoted by crystalline defects, while others occur preferentially on defect-free terraces. Different forms of structure sensitivity, and the underlying causes of this structure sensitivity, have been examined using several fuel-cell-relevant surface reactions in alkaline media as model reactions. Oxidation of CO serves as a model for defect favored reactions, while reduction of oxygen serves as a model for terrace favored reactions. More complicated reactions, such as methanol oxidation, can be interpreted as containing multiple steps that are either defect favored or terrace favored. The role of defects in each of these reactions was interpreted in terms of geometric and electronic effects, with different types of defects (kink type and step type) showing different effects for the different electrocatalytic processes. CO oxidation is promoted by both step-type and kink-type defects, as a result of electronic structure, but methanol dehydrogenation is promoted only by step-type defects, as a result of geometric structure.
 [DOI: 10.1149/1.2792335]

Manuscript submitted May 15, 2007; revised manuscript received September 6, 2007. Available electronically October 19, 2007.

Surface atoms with low coordination numbers, such as those at crystalline defects, possess enhanced activity for some catalytic reactions, as recognized originally by Taylor.[1] In experiments, as well as in theoretical modeling, the role of defects is often investigated through the use of stepped or otherwise defective monocrystalline surfaces.[2-11] Many surface reactions show a maximum in reactivity at an intermediate value of the step density. At low step density the steps may be too sparse to have a significant effect on reactivity, although in the case of rapid surface diffusion even a low defect density may be significant. At high step density, some reactions may be inhibited because they require an ensemble of surface sites larger than the terrace width. These effects have complicated efforts to determine the exact role of defects in catalytic processes.

The two main reasons for different activity at defects than at terraces are the modified geometric structure and the modified electronic structure at defects. The geometric structure at defects is significant because many reactions occur preferentially on specific atomic ensembles.[12,13] The modified electronic structure is significant because of the resulting effect on adsorption energies of reactants, products, and spectator species, as well as the effect on activation barriers.[14]

In order to evaluate defects as active sites in catalytic processes, we have prepared well-ordered Pt(111) surfaces, well-ordered Pt(10 10 9) surfaces, and lightly disordered Pt(111) surfaces with known distribution of defects accounting for $\approx 1\%$ of the total surface sites. We tested the catalytic activity of these surfaces in several reactions that are relevant to fuel cells. Based on these studies, we present an interpretation in which each reaction can be classified as either defect favored or terrace favored. Finally, we show how these classifications can be applied to complicated reaction mechanisms containing multiple series or parallel steps. A good understanding of the effects of surface structure on reactivity is paramount in the design of highly active catalytic surfaces, as well as in the optimization of existing catalysts. The results reported here are important for the understanding of catalytic processes in general, as well as for the understanding of the specific fuel cell electrocatalytic reactions investigated herein.

Experimental

All electrochemical experiments were performed with a 3 mm cylindrical Pt(111) electrode or a 2 mm cylindrical Pt(10 10 9) electrode. Materials used were: Ar, H_2, and CO (SJ Smith), H_2SO_4 (GFS), NaOH (Merck), and $AgNO_3$ (Aldrich). Electrochemical measurements were performed in a two-compartment cell with a Pt wire counter electrode. The reference electrode, a Ag/AgCl electrode (BAS), was immersed in 0.1 M H_2SO_4. The liquid-liquid junction between H_2SO_4 and NaOH solutions occurred in the Luggin capillary connecting the reference compartment to the main compartment of the cell. The electrode was calibrated several times in situ vs a reversible hydrogen electrode (RHE) in the main cell compartment, thus correcting for the junction potential. The potential difference was always stable during extended tests. Using this procedure, the OH desorption peak on Pt(111) was found to occur at precisely 0.763 V vs RHE. This feature was used as an internal reference to compensate for any possible drifts in the reference potential during the measurements. All potentials are quoted vs RHE. An Autolab PGSTAT 30 potentiostat was used for all electrochemical measurements.

Full details of the experimental procedure are given elsewhere.[15] Briefly, the clean electrode was annealed in a H_2 flame and cooled in H_2 + Ar, then covered with a drop of water for transfer to the electrochemical cell. After potential cycling in 0.1 M H_2SO_4, the electrode was rinsed with Ar-purged water and the solution was replaced with Ar-purged 0.1 M NaOH, all under a continuous Ar blanket. Adsorption of CO was performed at 0.10 V by introducing a stream of CO into the Ar blanketing gas while the electrode was maintained in meniscus configuration. Ar-purged methanol was added to the solution using a glass and polytetrafluoroethylene (PTFE) syringe through a PTFE needle inserted into the cell from the top. After methanol oxidation, the CO coverage was measured by voltammetry in methanol-free solution. The solution exchange was performed by introducing a small amount of H_2 gas into the Ar blanketing stream, draining the solution, rinsing the cell and the electrode with methanol-free 0.1 M NaOH, eliminating the H_2 stream, and immersing the electrode in fresh solution.

Scanning tunneling microscopy (STM) was performed in situ in 0.1 M NaOH solution using a Molecular Imaging Pico STM. A 1 cm cylindrical Pt(111) crystal was used for STM. The crystal was annealed in a H_2 flame, cooled in Ar + H_2, and protected by adsorption of iodine from 1 mM KI solution for transfer to the STM cell. After the transfer, the adsorbed iodine was removed by holding the potential at approximately 0.1 V while rinsing with 0.1 M NaOH. Imaging was performed in constant current mode with a tunneling

* Electrochemical Society Student Member.
** Electrochemical Society Active Member.
[a] Present address: MPA-11, Los Alamos National Laboratory, Los Alamos, NM 87545, USA
[z] E-mail: andrzej@scs.uiuc.edu

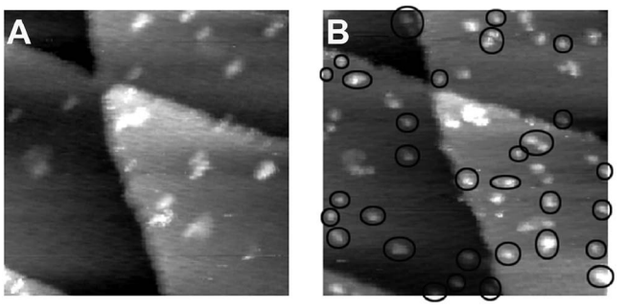

Figure 1. 40 × 40 nm in situ STM images of Pt(111) in 0.1 M NaOH. (A) Freshly annealed Pt(111) surface at 0.1 V. (B) Same surface at 0.1 V after holding at 1.25 V for 10 s. Circles mark islands formed by the potential step. Tip potential=0.9 V.

current of 1–2 nA. Electrochemically etched Pt–Ir tips, coated with paraffin wax, were used for the STM measurements, and a Ag/AgCl electrode was used as the reference electrode.

Results and Discussion

The roles of defects in catalytic reactions can be probed by introducing a small defect density on an otherwise well-ordered monocrystalline surface. In this study two kinds of defects were examined: (110) steps, present on a Pt(10 10 9) surface, and Pt islands, which were produced by lightly disordering a Pt(111) surface. A small number of islands are present even on a freshly annealed Pt(111) surface (Fig. 1A), but stepping the potential to 1.25 V for 10 s greatly increases the island density (Fig. 1B). The circles in Fig. 1B mark islands that appeared following the potential step, while the unmarked islands were already present before the potential step. All of the islands produced by the disordering treatment are monatomic in height and under 2 nm in diameter, while 90% of these islands are 1 nm in diameter or less. These small islands have predominantly kink-type adsorption features, unlike the step-type features present on larger Pt islands.[15]

At low density, defects do not interfere with processes occurring on terraces, but act as active sites for certain catalytic processes. On surfaces with a low defect density, simple catalytic reactions can be divided into two categories: reactions that occur preferentially at defects, and reactions that occur preferentially on terraces. Defect-favored reactions can be further categorized by the types of defects that promote them. This categorization is illustrated for several reactions in Table I.

Defect-favored reactions.— Reactions may occur preferentially at defects because of geometric effects, electronic effects, or both. The role of electronic structure will be considered first. The position of the d band center has been shown to be particularly important in determining metal-adsorbate bond strength.[16] The strong interaction of adsorbate states with the metal d band causes splitting into bonding and antibonding states. At defect sites, such as the small Pt islands of Fig. 1B, the decreased coordination number of the metal atoms causes narrowing of the d band, and a resultant upshift of the d band center. The upshift in the adsorbate-metal d states causes an increasing proportion of the antibonding states to move above the Fermi level, leading to stronger metal-adsorbate bonding, and hence higher adsorbate coverage, at defect sites. Reactions limited by low coverage of one of the reactant species can be accelerated by the increased reactant coverage on defect-rich surfaces. The CO oxidation reaction on Pt(111) may be considered as a model of this type of reaction. Oxidation of CO on Pt(111) in alkaline solutions has been shown to proceed through a Langmuir-Hinshelwood (L-H) mechanism.[15] The rate-limiting step in this reaction is a chemical step (Eq. 1)

$$CO_{ad} + OH_{ad} \rightarrow COOH_{ad} \quad [1]$$

$COOH_{ad}$ is rapidly removed through Eq. 2

$$COOH_{ad} + OH_{ad} \rightarrow CO_2 + H_2O \quad [2]$$

Equation 2 is followed by conversion of CO_2 in solution to CO_3^{2-}, so the overall CO oxidation reaction can be written as Eq. 3

$$CO_{ad} + 4\,OH^- \rightarrow CO_3^{2-} + 2H_2O + 2e^- \quad [3]$$

At high CO coverage, the rate of Eq. 1 is controlled by the coverage of OH. In the low potential region of interest for fuel cell applications, OH adsorption on Pt(111) terraces is negligible, so CO oxidation is limited to defect sites. Increasing the defect density by lightly disordering a Pt(111) surface, which produces a surface like the one depicted in Fig. 1B, substantially enhances CO oxidation at low potential (Fig. 2A). Surfaces such as that shown in Fig. 1B are stable even upon transfer to sulfuric acid solutions, similarly resulting in enhanced CO oxidation in this acidic environment.[15] The defects produced in the disordering process, which have adsorption properties similar to those of kink sites,[15] act as adsorption sites for OH, with the higher OH coverage leading to accelerated CO oxidation. The 150% acceleration of CO oxidation in alkaline media at a defect density around 1% (defect density determined from the adsorption feature at 0.49 V in the cyclic voltammogram in Fig. 2B) attests to the prominent role of defects in CO oxidation, as well as to the rapid diffusion of CO across terraces to defect sites.[17,18] Indeed, the enhancement due to defects is much larger than that indicated by Fig. 2A, since the reactivity of the well-ordered Pt(111) surface is controlled by the native defect density. Even the very low level of defects on the well-ordered surface, caused by crystal miscut and imperfections in the annealing/cooling/transfer process, is still enough to dominate the activity for CO oxidation at low potential. This conclusion is supported by the poor reproducibility of the CO oxidation prepeak and the sensitivity of this feature to adsorption processes that block surface defects.[15] For instance, defect blockage by Ag leads to a major suppression in the CO oxidation activity at low potential. Pt(111)/Ag surfaces were prepared by Ag electrodeposition on the Pt(111) surface by cyclic voltammetry between 0.05 and 0.85 V in a 1 μM $AgNO_3$ + 0.1 M NaOH solution. After formation of a partial Ag monolayer, the electrode was transferred to 0.1 M H_2SO_4 under an Ar blanket and cycled between 0.05 and 0.85 V until the Ag coverage had decreased to 0.10 ML (as determined by suppression of H adsorption[19]), then transferred back to 0.1 M NaOH for CO oxidation. The resulting partial Ag monolayer selectively blocks defects,[20] preventing OH adsorption on these sites, but it does not strongly affect adsorption processes occurring on terraces (Fig. 2B). Oxidation of CO on this Pt(111)/Ag surface occurs at a rate ~25 times lower than the rate on Ag-free Pt(111), as shown in Fig. 2A. This observation may be taken as further confirmation that CO oxidation at low potentials on Pt(111) is limited to defect sites.

Step-type defects also enhance CO oxidation on Pt(111), but with some mechanistic differences from kink-type defects. As shown in Fig. 2A, potentiostatic oxidation of adsorbed CO on a Pt(10 10 9) surface produces an initial current that is not significantly different from that of a well-ordered Pt(111) surface. At longer times, a peak develops in the current transient, signaling

Table I. Favored sites for reactions on Pt(111) in alkaline media.

	Favored site		
	Terrace	Kink	Step
CO oxidation ($\theta_{CO} > 0.20$ ML)		✓	✓
CO oxidation ($\theta_{CO} < 0.20$ ML)	✓		
Oxygen reduction	✓		
Methanol dehydrogenation			✓

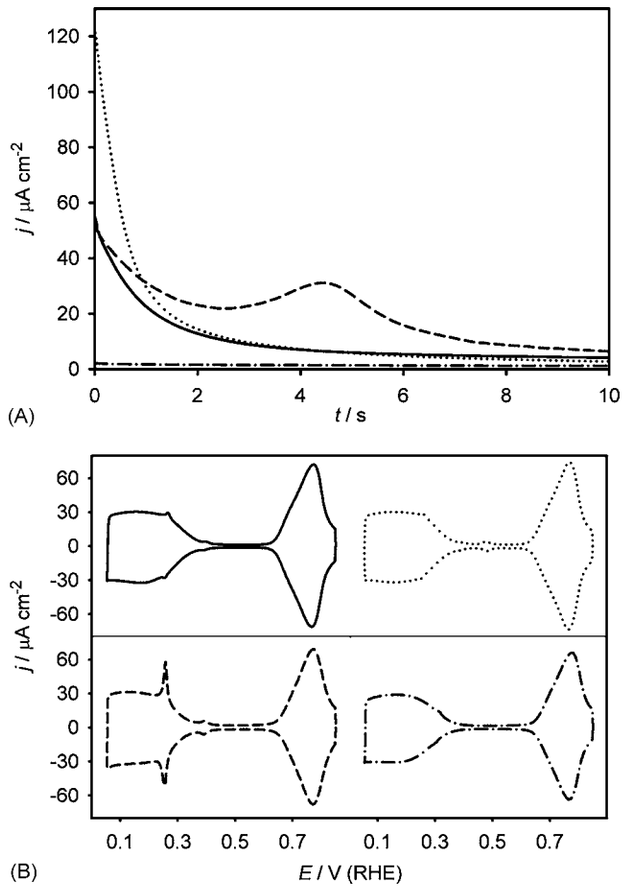

Figure 2. (A) Potentiostatic oxidation of a saturated CO adlayer (0.69 ML) at 0.55 V in 0.1 M NaOH. (B) Background cyclic voltammograms for each of the surfaces in (A). Solid line: well-ordered Pt(111); dotted line: Pt(111) lightly disordered by holding at 1.25 V for 10 s; dashed line: Pt(10 10 9); dot-dash line: Pt(111)/Ag (0.10 ML Ag).

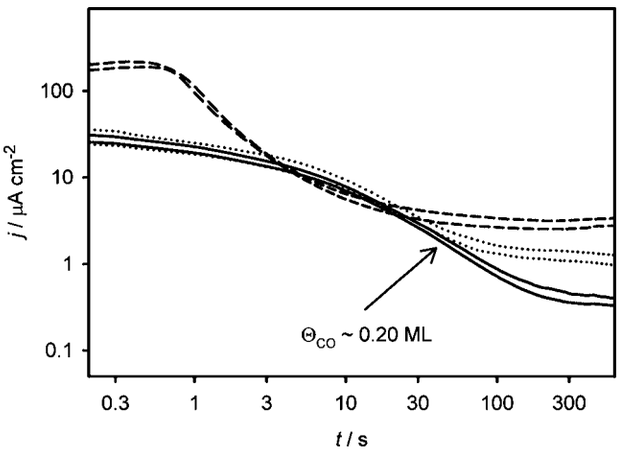

Figure 3. Oxidation of 0.1 M methanol at 0.45 V on an initially CO-free surface in 0.1 M NaOH. Solid lines: well-ordered Pt(111); dotted lines: lightly disordered Pt(111); dashed lines: Pt(10 10 9). Lines represent upper and lower bounds of 95% confidence intervals. The arrow indicates the point at which θ_{CO} = 0.20 ML on well-ordered Pt(111).

competitive adsorption of CO and OH. Thus, (110) steps enhance CO oxidation, but only once CO has been removed from them so that OH can adsorb. In contrast, potentiostatic oxidation of CO on a lightly disordered Pt(111) surface with kink-type defects produces a monotonically decaying current transient, indicating that CO and OH do not compete for adsorption sites under these conditions. Indeed, we previously found that CO and OH only compete for adsorption at kink-type defects at the highest CO coverage.[15] Attainment of this CO coverage only occurs when CO is dissolved in solution.[21]

Although the results reported here are in agreement with studies of CO oxidation in acidic media, which have found a correlation between defect density and CO oxidation rate,[3] they are in disagreement with analyses by other workers, which have shown a negligible correlation between defect density and rates of various catalytic reactions.[22] The reported inability of defects to promote reactivity was attributed to local relaxation at defects, which would mitigate the perturbations in coordination number and electronic structure. Despite these arguments, ample evidence exists for stronger adsorption at defect sites,[14,23-29] and in the case of OH adsorption this leads to enhanced CO oxidation kinetics on a variety of defective metal surfaces.[15,18,30-32]

Although CO oxidation on Pt(111) in alkaline media has been shown to serve as a model of a defect-favored reaction at high CO coverage, the situation changes considerably at CO coverage lower than 0.20 ML. In this case a shift in mechanism occurs, causing CO oxidation to become a terrace-favored reaction, as discussed in the next section of this paper.

In contrast to CO oxidation, which is defect favored because of electronic structure effects, the results presented here indicate that methanol dehydrogenation to CO on Pt(111) in alkaline solutions serves as an example of a reaction that is defect favored because of geometric structure effects. Since in alkaline media CO oxidation does not occur at low potential when the CO coverage is lower than 0.20 ML,[15] the initial current during potentiostatic methanol oxidation corresponds only to methanol dehydrogenation. As reported earlier,[33,34] Pt(111) has by far the lowest activity of the three basal Pt surfaces for methanol dehydrogenation. Therefore, adding defects with (110) orientation, such as the steps on a Pt(10 10 9) surface, provides favorably oriented Pt ensembles, greatly accelerating methanol dehydrogenation (dashed traces in Fig. 3). The effect of different types of defects on this reaction is particularly notable. While (110) steps have favorable geometry for methanol dehydrogenation, very small Pt islands (diameter ~1 nm), which are characterized by kink-type adsorption sites,[15] have no significant effect on methanol dehydrogenation (dotted traces in Fig. 3). Since electronic structure perturbations at step-type and kink-type defects are similar in nature, both occurring as a result of decreased coordination number, this observation may be taken as further evidence that enhanced methanol dehydrogenation at (110) steps is caused by geometric effects.

Terrace-favored reactions.— Reactions that are hindered by excessively strong adsorption of a reactant, intermediate, product, or spectator species should not be accelerated by defects (as long as defects do not provide significantly more favorable geometry), since the defects serve to strengthen the adsorption. In the case of a spectator species, stronger adsorption leads to a higher coverage of the spectator species and a more complete site blockage. In the case of a reactant, stronger adsorption increases the activation barrier for reaction. In the case of an intermediate or a product, the reaction will be inhibited by slow removal of the strongly bound species. In each of these cases, defects will be deactivated. Therefore, this type of reaction occurs preferentially on terraces. The oxygen reduction reaction (ORR) on Pt(111) can be taken as a model of such a reaction. The ORR on Pt(111) is limited by strong adsorption of OH and O, decreasing the number of sites available for the ORR.[35] The notable hysteresis in Fig. 4, due to irreversible OH and O adsorption at high potentials, attests to the inhibiting effect of strongly adsorbed

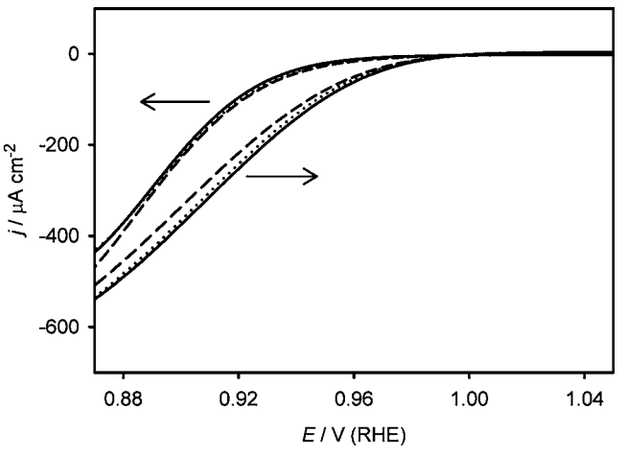

Figure 4. Cyclic voltammetry at 2 mV/s in O_2-saturated 0.1 M NaOH. Solid line: well-ordered Pt(111); dotted line: Pt(111) lightly disordered by holding at 1.25 V for 10 s to produce kink-type defects, followed by reduction at 0.10 V; dashed line: Pt(111) highly disordered by holding at 1.40 V for 10 s to produce step-type defects, followed by reduction at 0.10 V. The similarity of the traces demonstrates that defects do not play a significant role in O_2 reduction.

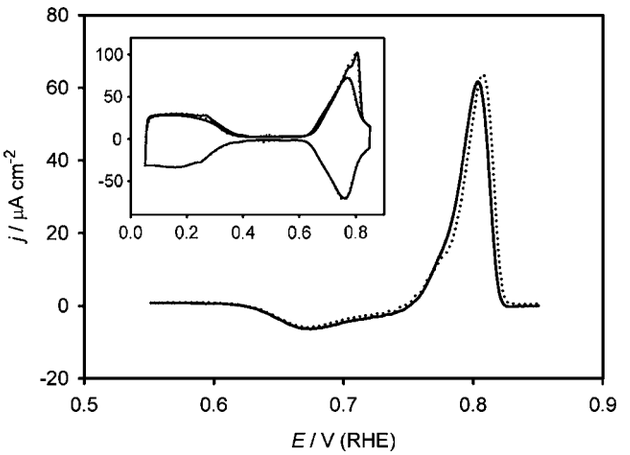

Figure 5. Oxidation of 0.06 ML of CO on Pt(111) surfaces. Inset shows CO stripping voltammograms superimposed on background voltammograms; the main figure shows CO stripping current with current from background voltammogram subtracted. Solid line: well-ordered Pt(111); dotted line: Pt(111) lightly disordered by holding at 1.25 V for 10 s.

O/OH.[36] Since these species adsorb more strongly on defects than on terraces, defects are mostly blocked in the potential range of interest for the ORR. Still, some Pt(111) terrace sites remain available for reaction, and since defects on surfaces such as the one shown in Fig. 1B account for only ~1% of surface sites, the activity of Pt(111) for the ORR does not change significantly with increasing defect density. Therefore, it may be concluded that the activity of defect sites for the ORR is no greater than that of terrace sites, and indeed, since the higher local d band center at defects causes them to be mostly blocked by adsorbed OH and O, they are probably less active than terrace sites. This interpretation is also in agreement with a study of the ORR on Pt(111) vicinal surfaces in $HClO_4$ solutions, which found a negligible correlation between activity and density of (111) steps as long as the terrace width was at least 9 atoms.[37] In contrast, a recent study of the Pt(111) surfaces with (100) steps revealed an enhancement in ORR activity with increasing step density in $HClO_4$,[38] suggesting that different types of defects may have different effects on ORR activity, although both types of defects investigated here (step type and kink type) were found to provide no ORR enhancement. As noted above, the low activity of defect sites for the ORR reported in this work most likely results from the higher d band center at defect sites. This interpretation is supported by observations of the ORR activity of Pt alloy catalysts. The lowering of the d band center caused by alloying Pt with other transition metals has been shown to increase ORR kinetics on Pt in acids, with smooth surfaces showing faster ORR rates than rough ones.[39]

Under some conditions, the CO oxidation reaction is also a terrace-favored reaction. Although CO oxidation on Pt(111) in alkaline solutions is a defect-favored reaction at CO coverage higher than 0.20 ML, at lower CO coverage the reaction mechanism undergoes a dramatic change, becoming a terrace-favored reaction similar to the ORR. The cause of this change lies in the coverage-dependent adsorption strength of CO. At high CO coverage, CO is relatively weakly adsorbed,[40,41] and can react with OH strongly adsorbed at defects. As the CO coverage decreases below 0.20 ML, CO becomes more strongly adsorbed, to the extent that it is no longer able to react with defect-bound OH, instead requiring more weakly bound OH on terraces. Thus, at low CO coverage, defects are blocked by strongly adsorbed and unreactive OH. Under these conditions, the rate of CO oxidation is no longer sensitive to the defect density (Fig. 5).

Complex surface reactions: Mixed terrace-favored and defect-favored steps.— The CO oxidation and O_2 reduction reactions discussed above may be considered as model reactions, representing patterns of structure sensitivity mirrored by other simple reactions. More complicated reactions do not necessarily conform to these simple categories, but can be considered as comprising multiple steps, in series or in parallel, that do conform to the defect-favored and terrace-favored reaction categories. The methanol oxidation reaction on Pt(111) in alkaline solutions is an example of such a reaction. The primary methanol oxidation pathway at potentials below 0.55 V involves methanol dehydrogenation through a series of C–H and O–H scission reactions, resulting in an adsorbed CO intermediate[42]

$$CH_3OH + 4\,OH^- \rightarrow CO_{ad} + 4H_2O + 4e^- \quad [4]$$

Subsequent CO oxidation, which occurs as described by Eq. 1 and 2, is negligible as long as the CO coverage is below 0.20 ML. Starting with a clean Pt(111) surface in 0.1 M NaOH + 0.1 M CH_3OH solution, approximately 40 s at 0.45 V is required to form 0.20 ML of CO.[15] Therefore, at times shorter than 40 s, Eq. 4 is the primary reaction. On this time scale, increasing the density of small Pt islands with kink-type adsorption sites (accomplished by lightly disordering the Pt(111) surface) has a negligible effect on the methanol dehydrogenation current (Fig. 3). This result demonstrates that methanol dehydrogenation on well-ordered and lightly disordered Pt(111) occurs primarily on terrace sites. Of course, we cannot completely exclude the participation of defect sites in the reaction, since at the low defect density of these surfaces (~1% or lower) the defects would have to be significantly more active than the terraces in order for an effect on the activity for methanol dehydrogenation to be observable. Still, at this defect density, kink-type defects do not contribute significantly to the overall activity of the surface.

In contrast to the results at short times, after 40 s of methanol oxidation at 0.45 V, the rate of methanol oxidation begins to show a marked dependence on the density of small Pt islands (Fig. 3). On this time scale, the CO coverage becomes higher than 0.20 ML, and CO oxidation starts to be significant, becoming the limiting factor as the CO coverage approaches the steady state value of about 0.28 ML on well-ordered Pt(111).[42] As discussed earlier, the need for defect sites in order to oxidize CO at low potentials causes the rate of CO oxidation to be sensitive to the defect density. Since methanol dehydrogenation is severely inhibited by increasing CO coverage, the

rate of methanol oxidation also becomes sensitive to the defect density at times longer than 40 s, as depicted in Fig. 3.

The discussion above demonstrates that methanol oxidation at low potential on well-ordered and lightly disordered Pt(111) in alkaline solutions, which consists of more than six elementary steps, can, as an approximation, be divided into a series of two steps, Eq. 4 followed by Eq. 3. The overall methanol oxidation reaction on these surfaces is therefore a series reaction in which the first step, methanol dehydrogenation, occurs on terraces, while the second step, CO oxidation, occurs at defects. The situation is somewhat different on Pt(10 10 9). On this surface, (110) steps promote methanol dehydrogenation. Thus, on vicinal Pt(111) surfaces, methanol oxidation can be considered as a series reaction in which both steps are defect favored.

Conclusion

Many catalytic processes occurring on well-defined surfaces can be categorized as either defect favored or terrace favored. Defects may influence reactivity through geometric effects, related to the presence of specific ensembles of surface atoms in favorable positions for catalytic promotion, or through electronic effects, related to the ability of alterations in electronic structure at defects to affect adsorbate coverage and to stabilize activated states. Reactions in which electronic effects are more significant than geometric effects will tend to be defect favored if they are limited by insufficient adsorption of a reactive species, or terrace-favored if they are limited by excessively strong adsorption, whether of a reactive species or a spectator species.

Oxidation of CO at high coverage and low potential on Pt(111) in alkaline media serves as a model of a defect-favored reaction, in which the role of defects is to stabilize adsorbed OH at lower potential than on terraces. Reduction of oxygen on Pt(111) in alkaline media serves as a model of a terrace-favored reaction, in which defects are deactivated by strong localized adsorption of OH/O, leaving terrace sites as the active sites. Several other reactions occurring on Pt(111) in alkaline solutions, including CO oxidation at low CO coverage and methanol dehydrogenation, also conform to the defect-favored/terrace-favored categorization. The method of analysis laid out above can be used to describe even more complicated reactions such as the total methanol oxidation reaction on Pt(111) in alkaline media. Our analysis demonstrates that this reaction can be thought of as a series of two steps. The first step, methanol dehydrogenation, is terrace favored on well-ordered and lightly disordered Pt(111), but defect favored on vicinal Pt(111) surfaces with (110) oriented steps. The second step, CO oxidation, is defect favored on all Pt(111) surfaces.

Understanding the role of defects is necessary for the rational design of heterogeneous catalysts that exploit surface structure to increase activity. The analysis described herein is helpful in understanding limiting processes for all structure-sensitive catalytic processes, as well as for the understanding of the specific fuel cell catalysis reactions we have discussed.

Acknowledgments

This work is supported by the U.S. Army Research Office under DDD grant no. DAAD19-03-1-0169 and by the U.S. Department of Energy under grant no. DE-FG02005ER46260. Part of this work was supported by a CAREER award from NSF-CTS to P.J.A.K. J.S.S. acknowledges support from a NSF Graduate Research Fellowship and from NSF grant no. CHE 03-49999.

University of Illinois at Urbana-Champaign assisted in meeting the publication costs of this article.

References

1. H. S. Taylor, *Proc. R. Soc. London, Ser. A*, **108**, 105 (1925).
2. A. Szabo, M. A. Henderson, and J. T. Yates, *J. Chem. Phys.*, **96**, 6191 (1992).
3. N. P. Lebedeva, M. T. M. Koper, J. M. Feliu, and R. A. van Santen, *J. Phys. Chem. B*, **106**, 12938 (2002).
4. A. V. Tripkovic and K. D. Popovic, *Electrochim. Acta*, **41**, 2385 (1996).
5. N. Hoshi, E. Sato, and Y. Hori, *J. Electroanal. Chem.*, **540**, 105 (2003).
6. M. D. Macia, E. Herrero, J. M. Feliu, and A. Aldaz, *J. Electroanal. Chem.*, **500**, 498 (2001).
7. S. G. Sun and Y. Lin, *Electrochim. Acta*, **44**, 1153 (1998).
8. A. Scheibe, M. Hinz, and R. Imbihl, *Surf. Sci.*, **576**, 131 (2005).
9. T. Li, B. Bhatia, and D. S. Sholl, *J. Chem. Phys.*, **121**, 10241 (2004).
10. I. M. Ciobica and R. A. van Santen, *J. Phys. Chem. B*, **107**, 3808 (2003).
11. G. Samjeske, X. Y. Xiao, and H. Baltruschat, *Langmuir*, **18**, 4659 (2002).
12. F. Maroun, F. Ozanam, O. M. Magnussen, and R. J. Behm, *Science*, **293**, 1811 (2001).
13. S. Sugai, K. Shimizu, H. Watanabe, H. Miki, K. Kawasaki, and T. Kioka, *Surf. Sci.*, **287**, 455 (1993).
14. B. Hammer, *Top. Catal.*, **37**, 3 (2006).
15. J. S. Spendelow, J. D. Goodpaster, P. J. A. Kenis, and A. Wieckowski, *J. Phys. Chem. B*, **110**, 9545 (2006).
16. B. Hammer and J. K. Norskov, *Adv. Catal.*, **45**, 71 (2000).
17. T. Kobayashi, P. K. Babu, L. Gancs, J. H. Chung, E. Oldfield, and A. Wieckowski, *J. Am. Chem. Soc.*, **127**, 14164 (2005).
18. N. P. Lebedeva, M. T. M. Koper, J. M. Feliu, and R. A. van Santen, *J. Electroanal. Chem.*, **524**, 242 (2002).
19. J. Clavilier, L. H. Klein, A. Vaskevich, and A. A. ElShafei, *J. Chem. Soc., Faraday Trans.*, **92**, 3777 (1996).
20. P. Gambardella, M. Blanc, H. Brune, K. Kuhnke, and K. Kern, *Phys. Rev. B*, **61**, 2254 (2000).
21. A. Lopez-Cudero, A. Cuesta, and C. Gutierrez, *J. Electroanal. Chem.*, **579**, 1 (2005).
22. L. P. Ford, P. Blowers, and R. I. Masel, *J. Vac. Sci. Technol. A*, **17**, 1705 (1999).
23. A. Teliska, W. E. O'Grady, and D. E. Ramaker, *J. Phys. Chem. B*, **109**, 8076 (2005).
24. P. J. Feibelman, S. Esch, and T. Michely, *Phys. Rev. Lett.*, **77**, 2257 (1996).
25. H. Wang, R. G. Tobin, D. K. Lambert, C. L. DiMaggio, and G. B. Fisher, *Surf. Sci.*, **372**, 267 (1997).
26. V. Johanek, S. Schauermann, M. Laurin, C. S. Gopinath, J. Libuda, and H. J. Freund, *J. Phys. Chem. B*, **108**, 14244 (2004).
27. A. D. Karmazyn, V. Fiorin, S. J. Jenkins, and D. A. King, *Surf. Sci.*, **538**, 171 (2003).
28. B. Hammer, *Surf. Sci.*, **459**, 323 (2000).
29. L. D. Burke, J. A. Collins, M. A. Horgan, L. M. Hurley, and A. P. O'Mullane, *Electrochim. Acta*, **45**, 4127 (2000).
30. T. H. M. Housmans and M. T. M. Koper, *J. Electroanal. Chem.*, **575**, 39 (2005).
31. A. M. El-Aziz and L. A. Kibler, *J. Electroanal. Chem.*, **534**, 107 (2002).
32. J. Lee, W. B. Wang, M. S. Zei, and G. Ertl, *Phys. Chem. Chem. Phys.*, **4**, 1393 (2002).
33. K. Franaszczuk, E. Herrero, P. Zelenay, A. Wieckowski, J. Wang, and R. I. Masel, *J. Phys. Chem.*, **96**, 8509 (1992).
34. E. Herrero, K. Franaszczuk, and A. Wieckowski, *J. Phys. Chem.*, **98**, 5074 (1994).
35. N. M. Markovic and P. N. Ross, in *Interfacial Electrochemistry*, A. Wieckowski, Editor, p. 821, Marcel Dekker, New York (1999).
36. N. M. Markovic, H. A. Gasteiger, and P. N. Ross, *J. Phys. Chem.*, **100**, 6715 (1996).
37. M. D. Macia, J. M. Campina, E. Herrero, and J. M. Feliu, *J. Electroanal. Chem.*, **564**, 141 (2004).
38. A. Kuzume, E. Herrero, and J. M. Feliu, *J. Electroanal. Chem.*, **599**, 333 (2007).
39. V. R. Stamenkovic, B. S. Mun, M. Arenz, K. J. J. Mayrhofer, C. A. Lucas, G. F. Wang, P. N. Ross, and N. M. Markovic, *Nat. Mater.*, **6**, 241 (2007).
40. G. Ertl, M. Neumann, and K. M. Streit, *Surf. Sci.*, **64**, 393 (1977).
41. Y. Y. Yeo, L. Vattuone, and D. A. King, *J. Chem. Phys.*, **106**, 392 (1997).
42. J. S. Spendelow, J. D. Goodpaster, P. J. A. Kenis, and A. Wieckowski, *Langmuir*, **22**, 10457 (2006).